Available online at www.eccomasproceedia.org
Eccomas Proceedia COMPDYN (2017) 3697-3710

ECCOMAS
Proceedia

COMPDYN 2017
6th ECCOMAS Thematic Conference on
Computational Methods in Structural Dynamics and Earthquake Engineering
M. Papadrakakis, M. Fragiadakis (eds.)
Rhodes Island, Greece, 15–17 June 2017

NUMERICAL STUDY ON SEISMIC RESPONSE ANALYSIS OF THE PLATE GIRDER BRIDGE DAMAGED BY THE 2016 KUMAMOTO EARTHQUAKE

MYA NAN AYE[1], AKIRA KASAI[2], and ZHIPENG LIU[1]

[1]Graduate School of Science and Technology, Civil and Environmental Engineering, Kumamoto University
Kurokami 2-39-1, Chuo-ku, Kumamoto City, 860-8555, Japan, Tel: 096-342-3579
e-mail: 154d9410@st.kumamoto-u.ac.jp, 169d8837@st.kumamoto-u.ac.jp

[2]Associate Professor, Faculty of Advanced Science and Technology, Division of Materials Science, Kumamoto University
Kurokami 2-39-1, Chuo-ku, Kumamoto City, 860-8555, Japan, Tel: 096-342-3579
e-mail: kasai@kumamoto-u.ac.jp

Keywords: Seismic response analysis, 2016 Kumamoto earthquake, Local buckling behavior, Damage survey, Tawarayama Bridge

Abstract. *In 2016 Kumamoto Earthquake, many buildings, embankment structures and transportation infrastructures have been damaged. This paper presents damage survey of a plate girder bridge, namely Tawarayama Bridge which is situated on Kumamoto Prefectural road No 28, Tawarayama bypass, where the damage related to the bridge is enormous and elucidates the damage mechanism that can occur in that type of bridge due to earthquake with epicenter which is very close to bridge.*

At first, the parts of Tawarayama Bridge are investigated in order to find out the damages and examine the factors of occurrence. Then, seismic response analysis of Tawarayama Bridge subjected to 2016 Kumamoto earthquake motion is carried out. In observing the damages, the local buckling behavior of steel main girders are found. So shell elements are applied in finite element model to consider local buckling behavior. Frequency analysis is carried out to grasp the vibration characteristics and after that, the time history response analyses are performed using earthquake ground motion in both longitudinal and transverse directions to investigate the dynamic response of the bridge. The predicted earthquake motion simulated by Professor Yoshiya Hata from Osaka University *is applied for dynamic response analysis. Finally, the results for comparison of numerical results with real disasters are discussed.*

Peer-review under responsibility of the organizing committee of COMPDYN 2017.
doi: 10.7712/120117.5676.17092

1 INTRODUCTION

On 2016 April 14, an earthquake of magnitude 6.5 (JMA seismic intensity of 7) hit the Kumamoto region, Japan. That earthquake is the fore shock followed by main shock which hit on 2016 April 16 with the magnitude of 7.3 (JMA seismic intensity of 7). There are more than 140 aftershocks within 2 days including at least 11 with magnitude of 4.5 and one with 6. Mashiki town and Higashi ward of Kumamoto are severely effected as the epicenters are located there. Due to the effect of these earthquakes, many buildings and transportation infrastructures are damaged.

2 SUMMARY OF EARTHQUAKE DATA

According to JMA (Japanese Meteorological Agency), 7 earthquakes with large intensity (4 with magnitude 5.4 to 5.9, 2 with 6.4 to 6.5 and one with 7.3) are occurred in same area from April 14 to 16. Table 1 shows the magnitude, maximum seismic intensity, ground surface acceleration and depth of two main shocks and Figure 1 is the location map of Kumamoto, Mashiki and Mount Aso.

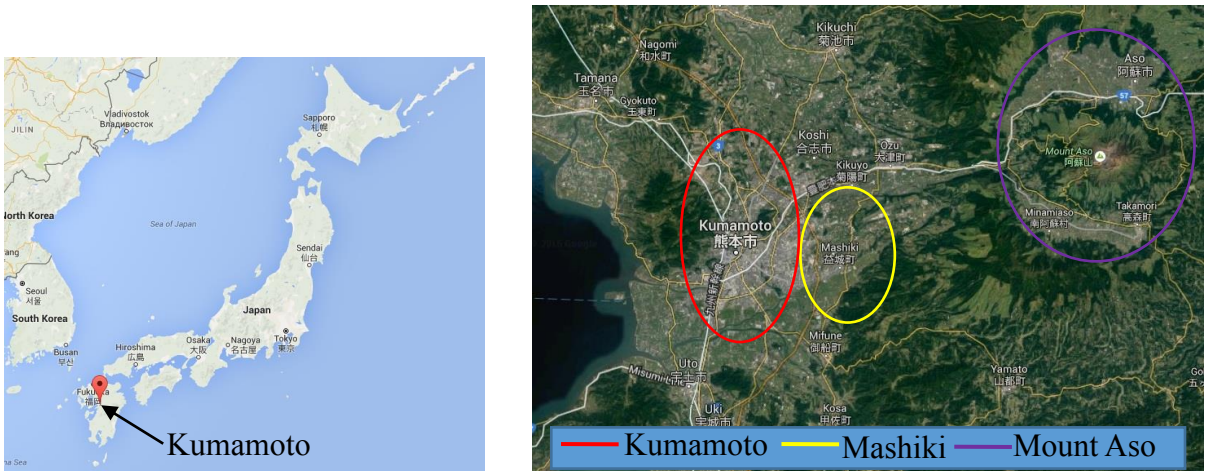

Figure 1. Location of Kumamoto, Mashiki and Mount Aso

Earthquake Name	Magnitude	Maximum Seismic Intensity	Acceleration (N-S or E-W)	Depth
2016 April 14, 21:26 (Fore Shock)	6.5	7 (Mashiki) 6 (Kumamoto)	925 cm/s^2 (Mashiki) 574 cm/s^2 (Kumamoto)	10 km
2016 April 16, 01:25 (Main Shock)	7.3	7 (Mashiki, Nishihara) 6 (Kumamoto)	1156 cm/s^2 (Mashiki) 827 cm/s^2 (Kumamoto)	10 km

Soure: JMA (Japan Meteorological Agency)

Table 1. Magnitude, Maximum Seismic Intensity, Acceleration and Depth of Main Shocks

3 OVERVIEW OF BRIDGE DAMAGES

Among 3000 bridges in Kumamoto Prefecture, about 40 bridges, including Aso Bridge and Minami-Aso Bridge, are severely affected by the earthquake and others 70 bridges under Kumamoto Prefecture administration are damaged also. Apart from these, JR Kyushu Shinkansen (Bullet Train) has been suspended due to damage of bridge on Kyushu Expressway.

Although most bridge piers are not damaged after foreshock, many bridges are severely damaged after main shock. In Kumamoto region, the phenomenon of pier settlements is found as characteristic damage. By looking the location of damage bridges on map, it is clear that most of the bridges that damaged are concentrated near fault.

Bridges on Tawarayama bypass which is an important route that connects the Kumamoto Prefecture and Miyazaki Prefecture are also damaged. This paper will mainly focus on damages of Tawarayama Bridge which is plate girder bridge and numerical study on seismic analysis of that bridge.

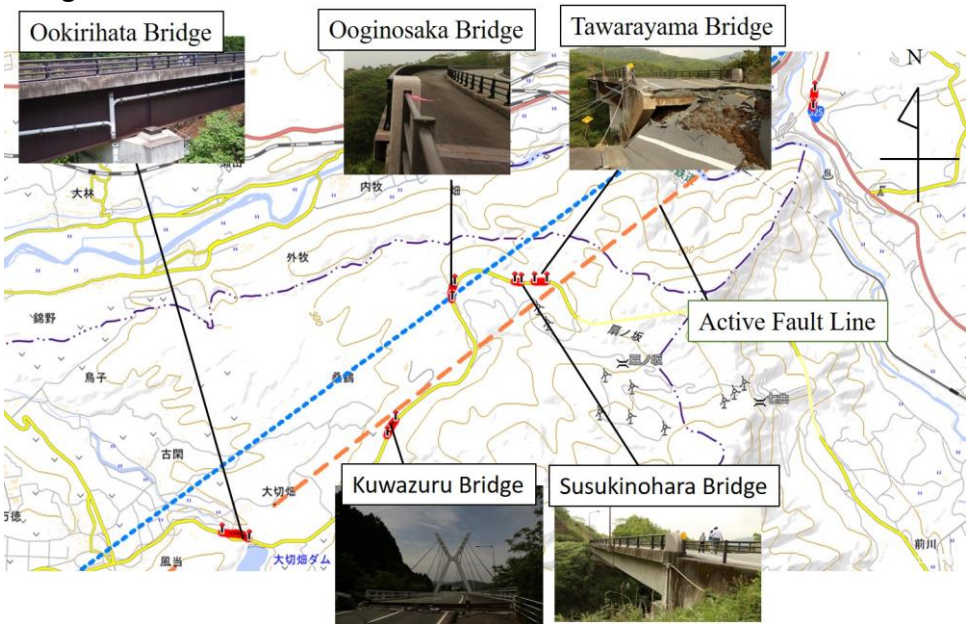

Figure 2. Location of damage bridges on Tawarayama bypass

4 OVERVIEW OF TAWARAYAMA BRIDGE

Tawarayama Bridge is a 3-span girder bridge of total length 140 m with maximum span length of 61.5m and effective width of 8.5 m. Substructure consists of inverted T type abutment (A1, A2) and overhang pier (P1, P2) and foundation consists of caisson pile. Figure 3 shows the longitudinal profile of the bridge. Figure 4 is the plan view of bridge in which A1 represents abutment of Kumamoto side and A2 represents that of Takamori side.

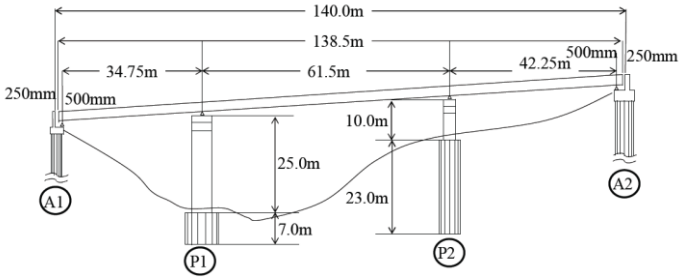

Figure 3. Longitudinal profile

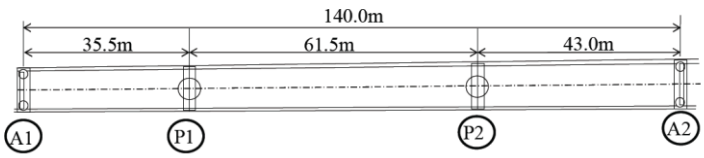

Figure 4. Plan view

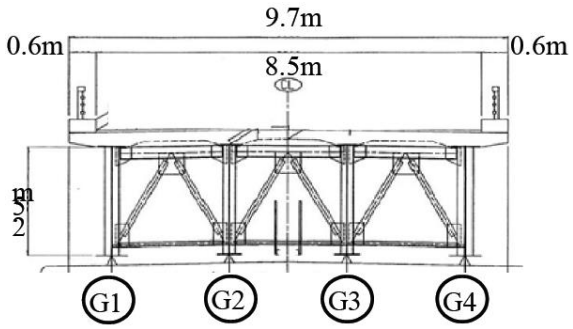

Figure 5. Cross section of superstructure

For the piers, it is represented as P1 and P2 from Kumamoto side. Figure 5 shows the cross-section of superstructure. A1 and A2 abutments are constructed as single column with deep foundation. The bridge is nearly straight and adopted the cable type girder prevention structure which connects the girder and the bridge abutment parapet as a bridge collapse prevention structures. Rubber bearing is used and side block is provided at the girder ends only.

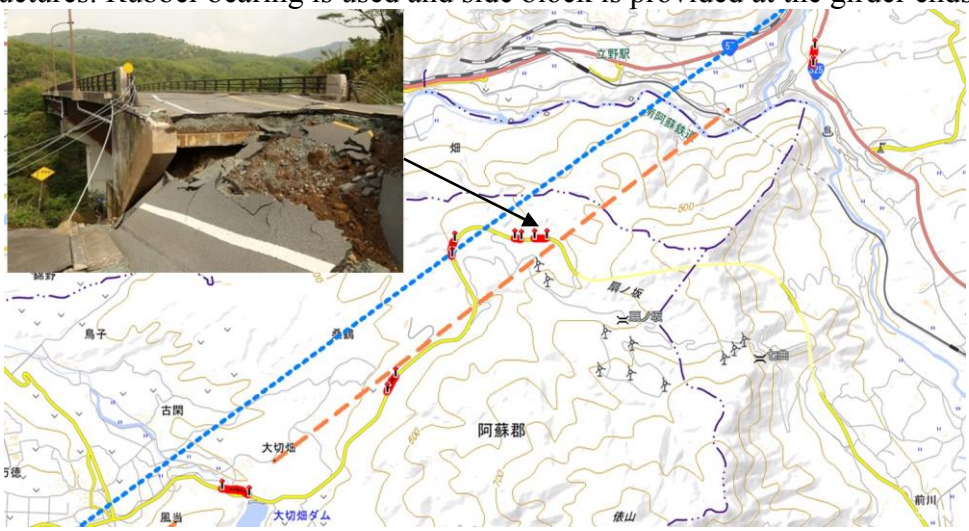

Figure 6. Location of Tawarayama Bridge

5 DAMAGE SURVEY OF TAWARAYAMA BRIDGE

Tawarayama Bridge which situate on Tawarayama bypass is also damaged by the 2016 Kumamoto earthquake as it is very near to active fault line. The deformation of the whole bridge can be seen in Figure 7 which was produced by 3D scanner technique. The damages of the bridge is found as follows.

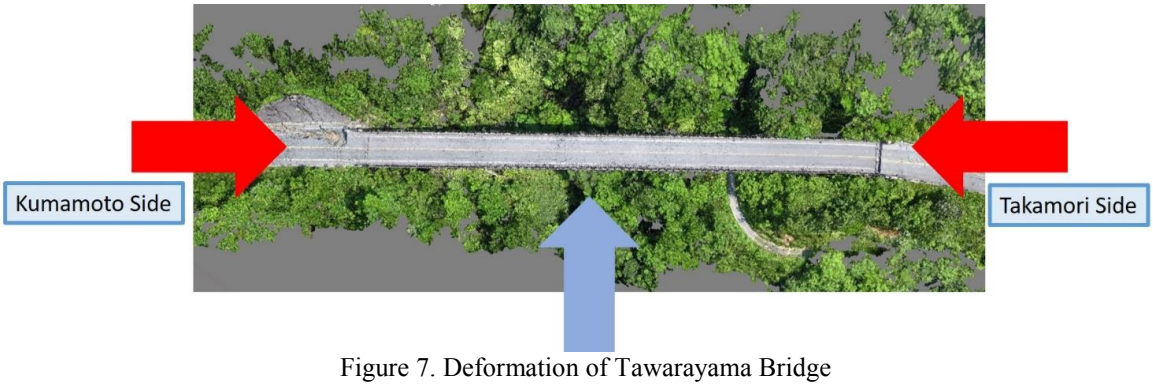

Figure 7. Deformation of Tawarayama Bridge

The settlement of deck slab is occurred at the east side (A2 side) of the bridge due to the girders falling off from the rubber bearings and the abutment tilting. The deck slab settlement of 53cm was seen as shown in Figure 8.

At the west side (A1 side), it is seen that road embankment has collapsed due to the soil movement and caused exposing of the pile foundation under the abutment. It may be due to large compressive force and future consideration should be made for specific result.

Figure 8. Damage of A2 abutment (East side)

Figure 9. Damage of A1 abutment (West side)

Figure 10. Deformation of main girder

Figure 10 shows the deformation of main girder and P1 pier seen from A1 side. The deformation can be found about 20 m from A1 side while moving towards P1. The deformation of G3 girder is shown in Figure 11. It has confirmed that the bucking in the vicinity of the lower lateral structure is occurred. The impinging of lower horizontal members buckling may be due to acting of compressive force on the bridge deck from both the A1 and A2 abutments, or, approaching of the abutments towards the bridge girder.

Figure 11. Deformation of girder 3

In this paper, this fact is raised as the most important destructive mechanism. The extent of compressive force which should be assumed for the seismic design of bridge girder, has not verified yet. In addition, the ground motion was larger than assumed so it is needed to identify the sites ground motion. According to this survey, it can be suggested that in future, seismic design of bridge girder should be considered based on the buckling phenomenon of bridge girder in response of seismic intensity 7 ground motion, especially at the vicinity of the girder ends.

6 SEISMIC RESPONSE ANALYSIS

ABAQUS software is used to create finite element model of Tawarayama Bridge. In this model, shell elements are applied to take account the local buckling behavior as such behavior of steel main girders are found in observing the damages. In addition, beam elements are used for considering whole buckling behavior. L-beam, T-beam and I-beam are used for cross-bracing, top and bottom chord, and cross-beams respectively. Solid elements for pier and abutment, and spring elements for bearing are applied in FE model. The material properties of the model used in the numerical analysis were, SM490 with yield stress (σ_y) of 400MPa and Young Modulus (E) of 205GPa for steel and concrete with Young Modulus (E) of 30.35GPa.

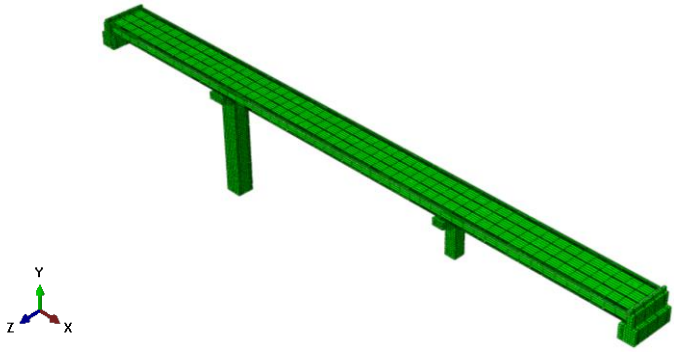

Figure 12. Finite Element Model of Tawarayama Bridge

6.1 Calculation of spring stiffness from properties of rubber bearing

In modeling Tawarayama Bridge, spring element is used for rubber bearing and the spring stiffness to be applied are calculated from properties of damper by using following formulae.

For horizontal direction,

$$K_{so} = (G_0 A)/(\Sigma t_e) \quad (1)$$

$$K_{st} = (G_0 A)/(\Sigma t_e) \quad (2)$$

For vertical direction,

$$K_v = (EA)/(\Sigma t_e) \quad (3)$$

where,

$$E = (3+6.58S^2)\ (0.5 \le b/a \le 2) \quad (4)$$

$$S = ab/(2(a+b)\ t_e) \quad (5)$$

$$E = (4+3.29S^2)\ (b/a<0.5,\ b/a>2) \quad (6)$$

$$S = a/2t_e \quad (7)$$

K_{so}, K_{st}, K_v = spring stiffness in horizontal and vertical direction
G_0 = shear modulus
A = area of rubber bearing
t_e = thickness of laminated rubber
E = Young's modulus
S = shape factor
a = width of rubber bearing
b = length of rubber bearing

The springs are installed at A1, P1, P2 and A2 between abutments or piers and girders. At each abutment and piers, 4 springs are installed under each girder. The values of each parameter used and calculated spring stiffness are shown in Table 2.

Part	G_0 (N/mm^2)	a (mm)	b (mm)	A (mm^2)	t_e (mm)	n	Σt_e (mm)	S	E (N/mm^2)	K_{so} (Nm/mm)	K_{st} (tf/cm)	K_v (tf/cm)
A1	0.785	450	450	202500	12	17	204	9.375	456.064	794.117	794.117	461637
P1	1.177	600	650	390000	22	5	110	7.091	392.883	4252.54	4252.54	1420410
P2	1.177	750	750	562500	36	3	108	5.208	213.555	6250	6250	1134190
A2	0.785	450	450	202500	13	11	143	8.654	388.961	1132.87	1132.87	561661

Table 2. Properties of rubber bearing and spring stiffness

6.2 Eigenvalue analysis

To grasp the vibration characteristics, the eigenvalue analysis was carried out. Natural periods and effective mass ratios of each predominant mode obtained from ABAQUS are presented in Table 3.

According to eigenvalue analysis result, it is observed that the 1st mode is translation in transverse direction (Z-axis), 2nd mode is vertical rotation, 3rd mode is translation in longitudinal direction (X-axis) and 4th mode is deflection. Maximum value of effective mass ratio for x, y and z component, longitudinal, tranverse and in plane direction, are found at mode 3, 9 and 1 respectively. That for x, y, z rotation are found at mode 8, 2 and 9.

MODE	Eigenvalue	Frequency (Cycle/time)	Effective Mass Ratio					
			X-component	Y-component	Z-component	X-rotation	Y-rotation	Z-rotation
1	33.829	0.92568	0.00000	0.00000	0.37221	0.03130	0.08588	0.00000
2	41.597	1.0265	0.00000	0.00000	0.26612	0.04693	0.71332	0.00000
3	42.606	1.0389	0.67256	0.00000	0.00000	0.00000	0.00190	0.00084
4	195.3	2.2242	0.00107	0.17451	0.00000	0.04119	0.00000	0.08490
5	202.44	2.2645	0.00000	0.00001	0.00008	0.00070	0.00009	0.00000
6	353.1	2.9907	0.00000	0.00000	0.11648	0.05998	0.03159	0.00000
7	410.55	3.2248	0.32490	0.00045	0.00000	0.00010	0.00094	0.00452
8	418.66	3.2565	0.00000	0.00000	0.17497	0.41388	0.04317	0.00000
9	611.62	3.9361	0.00058	0.35867	0.00000	0.08484	0.00000	0.73175
10	846.23	4.6298	0.00000	0.00000	0.00041	0.05812	0.00118	0.00000

Table 3. Eigen value analysis result

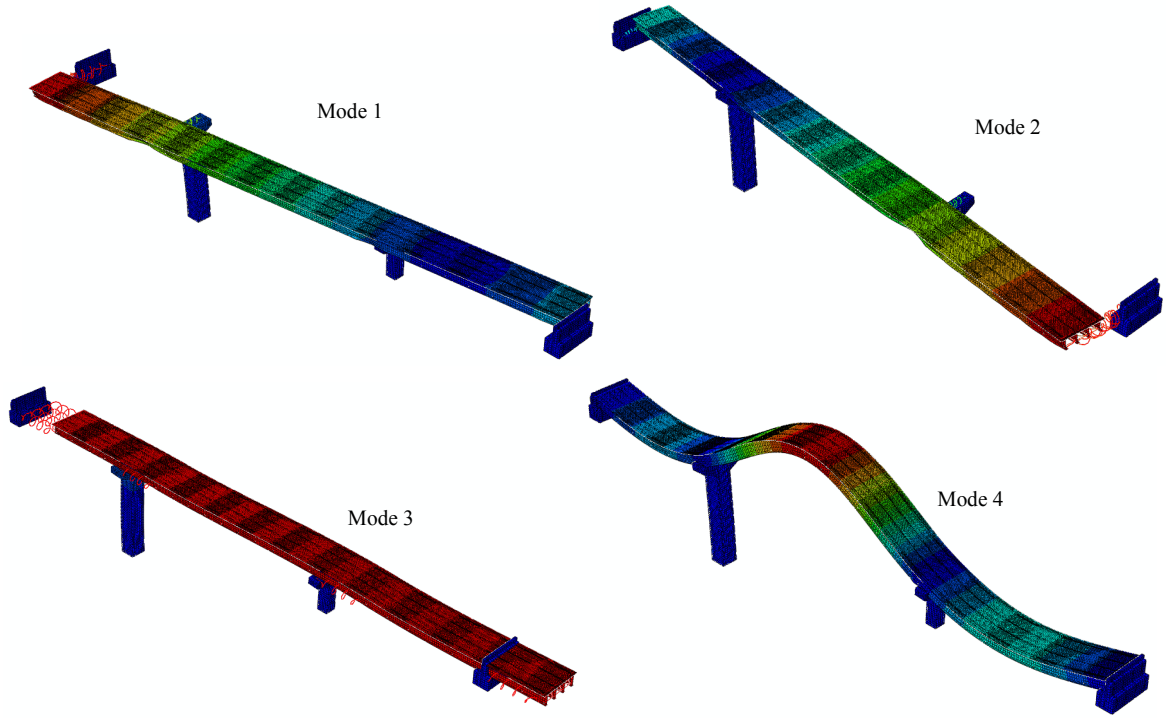

Figure 13. Mode shapes

6.3 Seismic input data

The predicted ground motion simulated by Professor Yoshiya Hata from Osaka University is used as seismic input data and that earthquake acceleration waves for East-West direction and North-South direction are illustrated in Figure 14 and 15. In Tawarayama Bridge, East-West is longitudinal direction and North-South is the transverse direction. Both longitudinal and transverse directions are considered to investigate the dynamic response of the bridge.

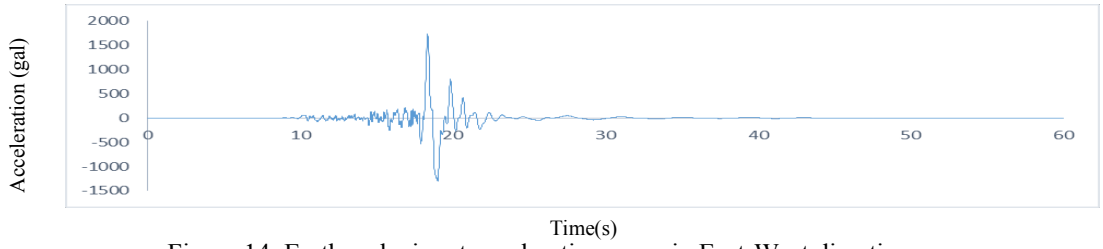

Figure 14. Earthquake input acceleration wave in East-West direction

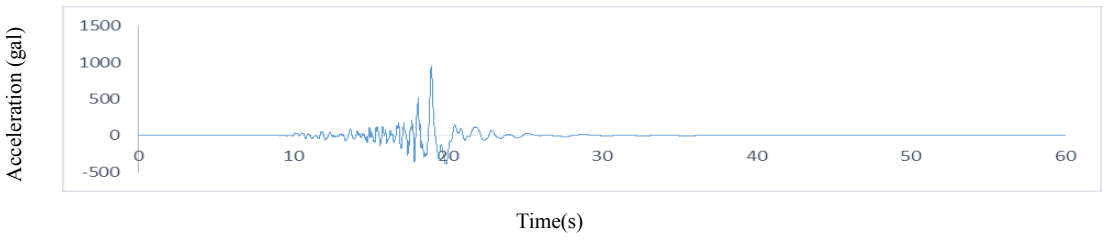

Figure 15. Earthquake input acceleration wave in North-South direction

6.4 Numerical analysis

For the numerical analysis, constant time step of 0.01sec is utilized. The seismic response analysis with ground acceleration input and a constant dead load is performed using the FEM ABAQUS program.

7 RESULTS AND DISCUSSION

7.1 Deformation of spring elements

This section will be discuss the deformation of spring elements used for rubber bearings. The load-displacement relationship curve of spring elements at each location are presented in longitudinal and transverse direction.

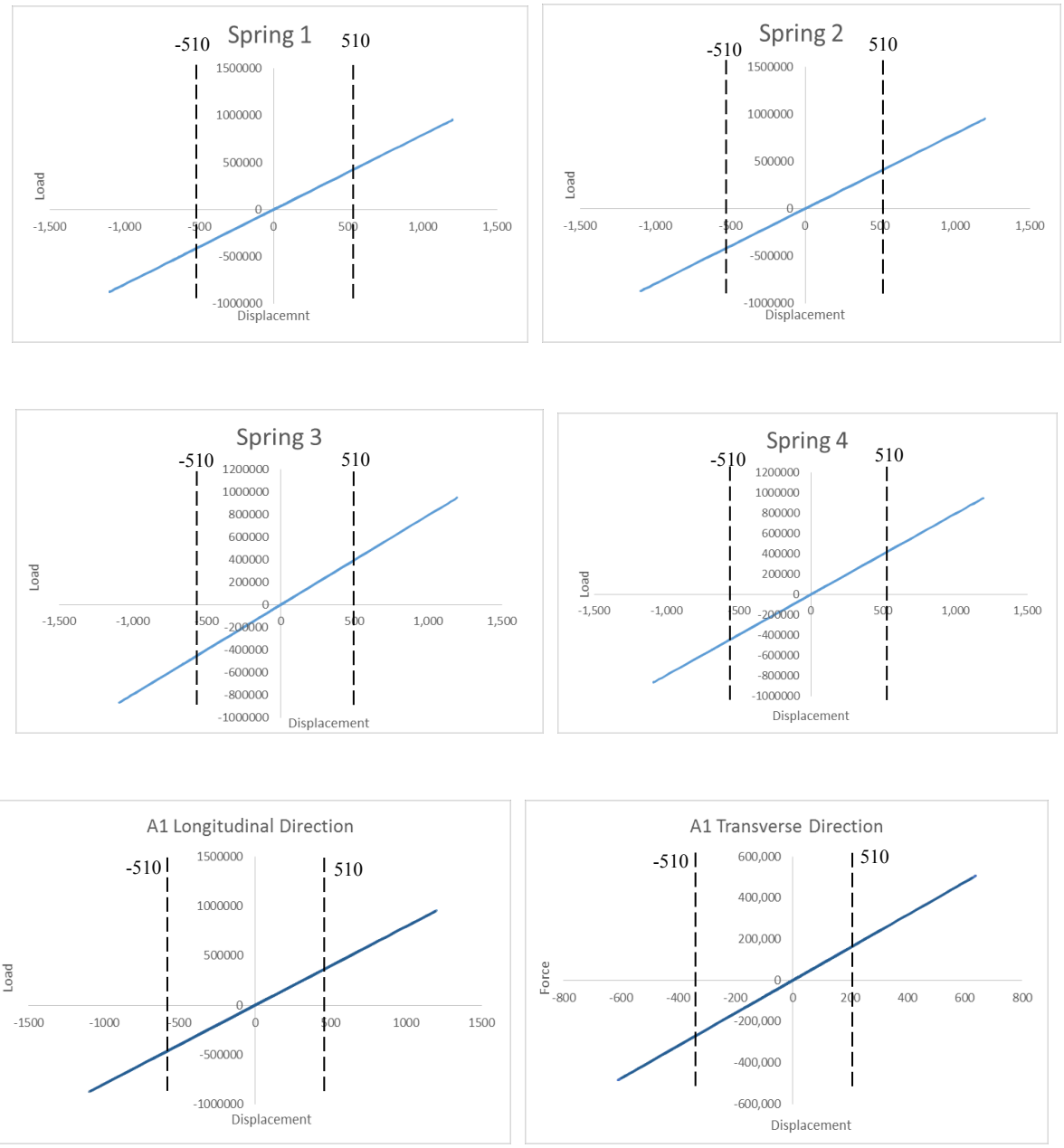

Figure 16. Stress-strain curves for spring at A1 abutment

The displacement in longitudinal direction found to be maximum for all springs. For the longitudinal direction, the value of displacement decrease from G4 to G1 in all A1, P1, P2 and A2. In transverse direction, the displacement decrease in the order G2, G3, G4 to G1 in abutments and decrease in order G2, G3, G1 to G4 in piers.

It is found that the displacement of all springs exceeds their displacement criteria except springs at P2 in transverse direction. The dotted lines in the Figure 16-19 shows the displacement criteria of spring elements from the theoretical point of view.

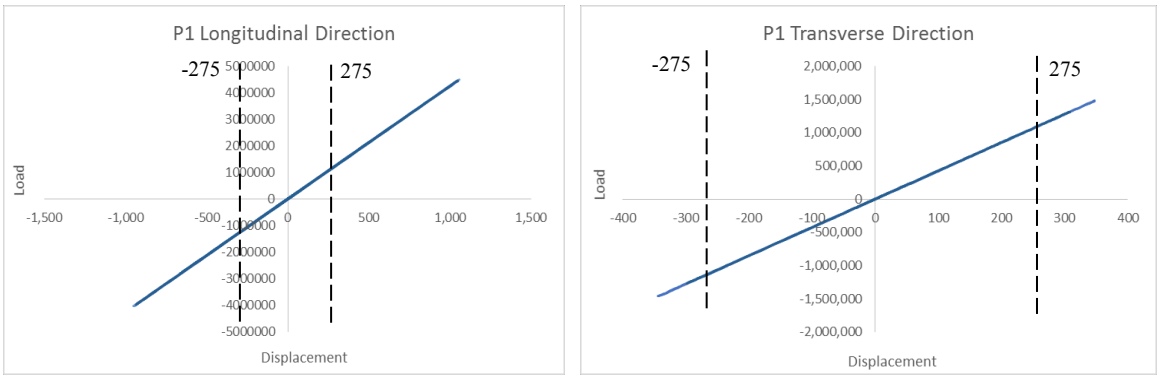

Figure 17. Stress-strain curves for spring at P1 pier

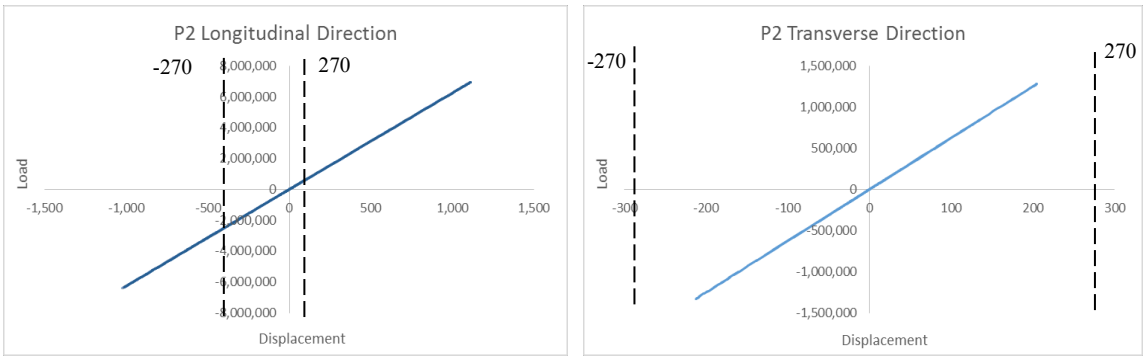

Figure 18. Stress-strain curves for spring at P2 pier

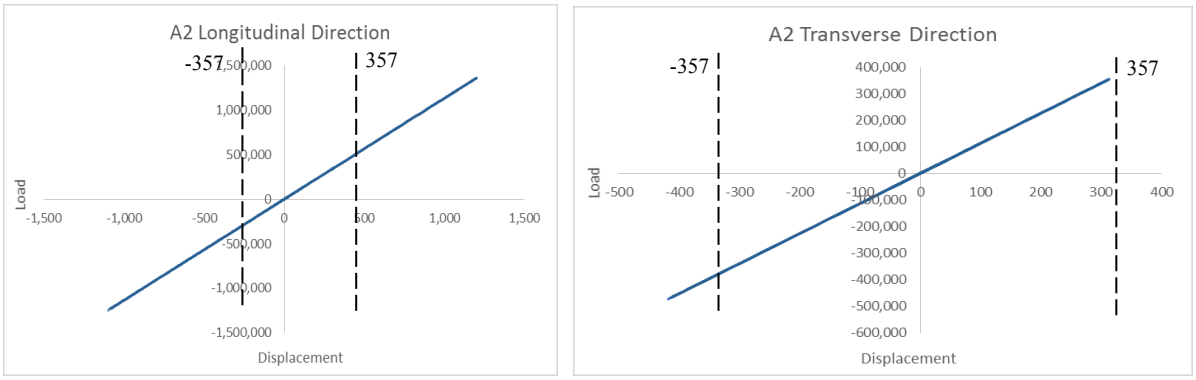

Figure 19. Stress-strain curves for spring at A2 abutment

7.2 Buckling of lower lateral members

Buckling of lower lateral members will be presented in this section. According to the Euler's buckling formula, buckling load can be presented by the following formula.

$$P_{cr} = \pi^2 EI/L_e^2 \quad (7)$$

The member section used for lower lateral members in Tawarayama Bridges is T 95 x 152 x 8 x 8 and the yield stress of the steel is 400 MPa. The following table describe the Euler's buckling loads according to the boundary conditions and the yield load of member used for lower lateral members.

	Pinned-Pinned	Fixed-Free	Fixed-Fixed	Fixed-Pinned
K	1	2	0.5	0.7
E (GPa)	205	205	205	205
I (mm^4)	4684000	4684000	4684000	4684000
L_e (mm)	2600	5200	1300	1820
A (mm^2)	1912	1912	1912	1912
Yield load (N)	764800	764800	764800	764800
P_{cr} (N)	1401922	350480	5607687	2861065

Table 4. Yield load and Euler's buckling according to boundary condition

Figure 20 shows the location of buckled members which are in most serious condition and labelled as 1 to 6 so as to clear for further explanation. These members are found buckled in actual condition also.

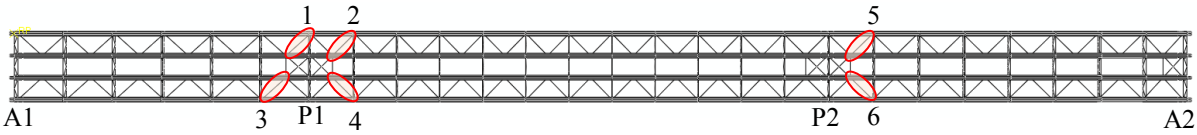

Figure 20. Location of buckled members

According to the displacement time history response, it is clear that displacement in longitudinal direction is greater than that in transverse direction. Displacement response according to time history is almost the same at ends and center position although noticeable differences are found in some members like in transverse direction of member 3 and 4. The maximum member forces of all members except member 1 in compression and tension are approximately 760000 N which is close to yield stress of the members. That of member 1 is around 400000 N which is much less than yield stress.

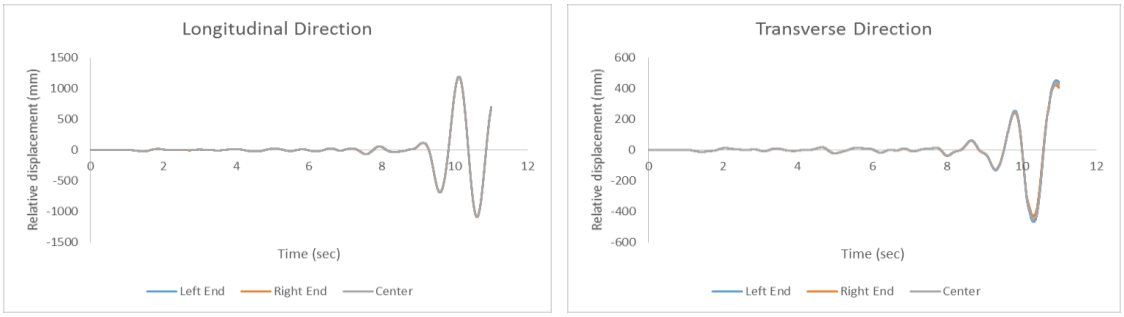

Figure 21. Displacement time history response of Member 1 in X and Y directions (Longitudinal and Transverse)

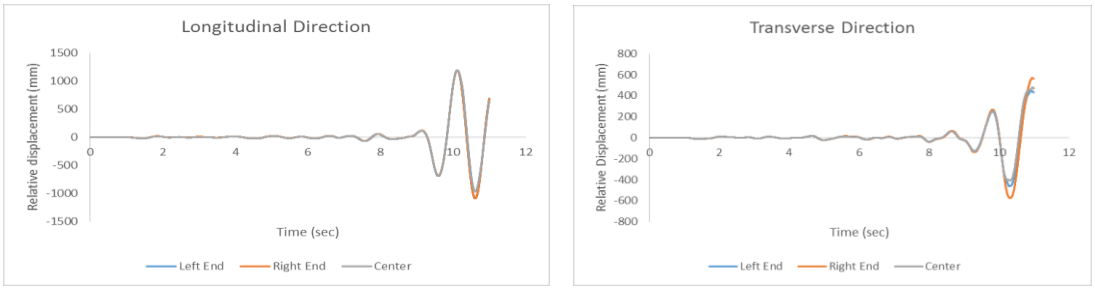

Figure 22. Displacement time history response of Member 2 in X and Y directions (Longitudinal and Transverse)

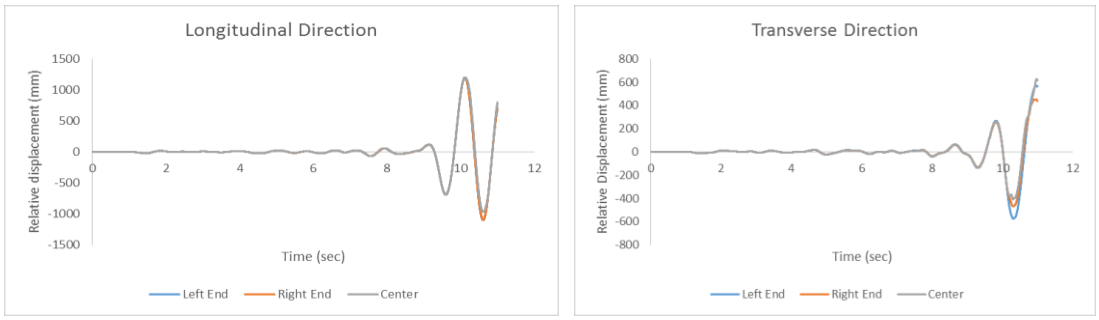

Figure 23. Displacement time history response of Member 3 in X and Y directions (Longitudinal and Transverse)

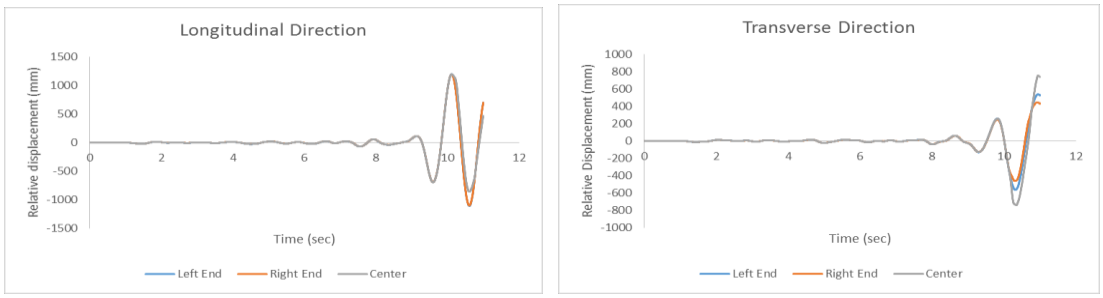

Figure 24. Displacement time history response of Member 4 in X and Y directions (Longitudinal and Transverse)

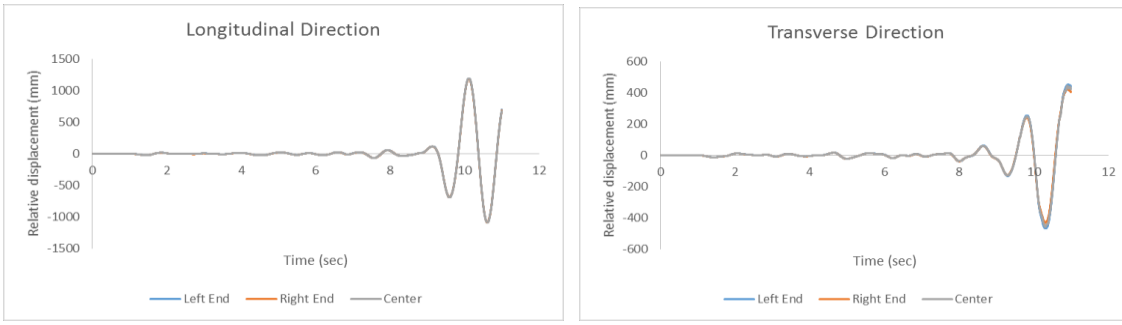

Figure 25. Displacement time history response of Member 5 in X and Y directions (Longitudinal and Transverse)

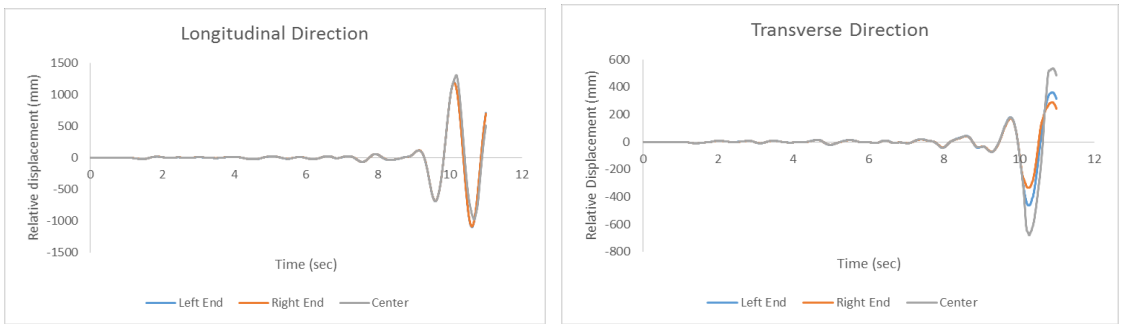

Figure 26. Displacement time history response of Member 6 in X and Y directions (Longitudinal and Transverse)

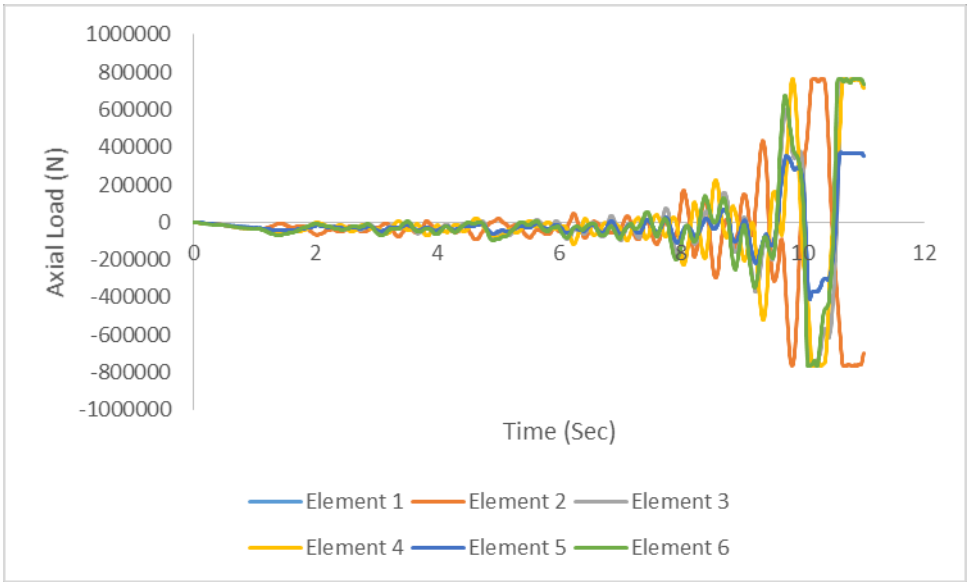

Figure 27. Load time history response in X and Y directions (Longitudinal and Transverse)

The load-deformation cure is too complex and the reasons for that behavior is under consideration. To investigate that behavior the simplify FE model using beam elements will be created in future.

8 SUMMARY AND CONCLUSIONS

Field surveys of Tawarayama Bridges are carried out to review the actual conditions and dynamic response analysis subjected to ground motion in longitudinal and transverse directions is also performed to investigate the seismic behavior of the bridge. The current findings and conclusions of this study are summarized as follows:

1. From field surveys
   - A large ground deformation near Tawarayama bridge
   - Moving of bridge towards Takamori side along longitudinal direction as well as towards valley side along transverse direction
   - Settlement of girder
   - Deformation of bridge girder due to compression force
   - Buckling of lower lateral members
   - Swaying of dampers and broken of damper
2. From dynamic response analysis
   - Displacement in both longitudinal and transverse directions (displacement in longitudinal direction is more dominant)
   - Deformation of main girder
   - Buckling of lower lateral members
   - Displacement of springs which exceeds the displacement criterial especially in longitudinal axis

By seeing these results, the following can be said that

- The displacement of bridge in real situation and the displacement results from dynamic analysis are similar although the values results from analysis is larger. This may due to inconsideration of contact between girder and abutment in FE model.
- In both field survey and analysis, the deformation of main girder near piers can be found.
- The lower lateral members that are buckled in real situation also shows buckling behavior during analysis.
- In actual condition, swaying of damper are more dominant in longitudinal direction and the spring elements used for rubber dampers displaced in longitudinal direction more than in transverse direction.

Even though, there are similar facts from field survey and dynamic response analysis, it is needed to upgrade the FE model for the following facts to get the better results.

- Applying fine mesh where thorough investigation is needed
- Considering contact behavior between main girders and abutments
- Considering damped condition

REFERENCES

[1] Dassault Systèmes Simulia Corp., Providence, RI, USA, ABAQUS 6.14 Documentation, 2014.

[2] Japan Road Association, Specifications for Highway Bridges, Part I - Steel Bridge and Part V - Seismic Design, Japan, 2002.

[3] Akira Kasai, Lessons from the 2016 Kumamoto Earthquake, Study Group of Structures in Tokai, The Symposium on considering how to keep bridges performance in Chubu region, pp 9-16, August, 2016.

[4] Akira Kasai, Mya Nan Aye, Damage survey of 2016 Kumamoto earthquake and the present state preservation in the suffered bridges using UAV, German Japanese Bridge Symposium 2016 (GJBS 2016), Osaka, Japan, August 30-31, 2016.

[5] Mya Nan Aye, Akira Kasai, Damage Survey of Bridges during the 2016 Kumamoto Earthquake and Numerical Analysis of Plate Girder Bridge subjected to the Kumamoto Earthquake, Japan-US Joint Workshop, The international Workshop on the 2016 Kumamoto Earthquake, Fukuoka, Japan, March 6, 2016.